

# Methane retrievals from Greenhouse Gases Observing Satellite (GOSAT) shortwave infrared measurements: Performance comparison of proxy and physics retrieval algorithms

D. Schepers,<sup>1</sup> S. Guerlet,<sup>1</sup> A. Butz,<sup>2</sup> J. Landgraf,<sup>1</sup> C. Frankenberg,<sup>3</sup> O. Hasekamp,<sup>1</sup> J.-F. Blavier,<sup>3</sup> N. M. Deutscher,<sup>4,5</sup> D. W. T. Griffith,<sup>5</sup> F. Hase,<sup>2</sup> E. Kyro,<sup>6</sup> I. Morino,<sup>7</sup> V. Sherlock,<sup>8</sup> R. Sussmann,<sup>9</sup> and I. Aben<sup>1</sup>

Received 1 February 2012; revised 12 April 2012; accepted 15 April 2012; published 30 May 2012.

[1] We compare two conceptually different methods for determining methane column-averaged mixing ratios ( $X_{\text{CH}_4}$ ) from Greenhouse Gases Observing Satellite (GOSAT) shortwave infrared (SWIR) measurements. These methods account differently for light scattering by aerosol and cirrus. The proxy method retrieves a  $\text{CO}_2$  column which, in conjunction with prior knowledge on  $\text{CO}_2$  acts as a proxy for scattering effects. The physics-based method accounts for scattering by retrieving three effective parameters of a scattering layer. Both retrievals are validated on a 19-month data set using ground-based  $X_{\text{CH}_4}$  measurements at 12 stations of the Total Carbon Column Observing Network (TCCON), showing comparable performance: for the proxy retrieval we find station-dependent retrieval biases from  $-0.312\%$  to  $0.421\%$  of  $X_{\text{CH}_4}$  with a standard deviation of  $0.22\%$  and a typical precision of 17 ppb. The physics method shows biases between  $-0.836\%$  and  $-0.081\%$  with a standard deviation of  $0.24\%$  and a precision similar to the proxy method. Complementing this validation we compared both retrievals with simulated methane fields from a global chemistry-transport model. This identified shortcomings of both retrievals causing biases of up to 1ings and provide a satisfying validation of any methane retrieval from space-borne SWIR measurements, in our opinion it is essential to further expand the network of TCCON stations.

**Citation:** Schepers, D., et al. (2012), Methane retrievals from Greenhouse Gases Observing Satellite (GOSAT) shortwave infrared measurements: Performance comparison of proxy and physics retrieval algorithms, *J. Geophys. Res.*, 117, D10307, doi:10.1029/2012JD017549.

## 1. Introduction

[2] Methane ( $\text{CH}_4$ ) is an important contributor to the anthropogenically enhanced greenhouse effect [*Intergovernmental*

*Panel on Climate Change*, 2007]. Monitoring its abundances in the Earth's atmosphere is one of the goals of the Greenhouse Gases Observing Satellite (GOSAT) [*Yokota et al.*, 2004; *Kuze et al.*, 2009]. The Fourier transform spectrometer on-board GOSAT (TANSO-FTS) operates in the shortwave infrared (SWIR) and thermal infrared (TIR) regions of the electromagnetic spectrum. The measurements in the shortwave infrared allow for the retrieval of  $\text{CH}_4$  column concentrations with high sensitivity at the Earth surface. Coupled with good spatial and temporal resolution, it can facilitate inverse modeling of methane sources and sinks.

[3] The use of space-based SWIR measurements for inverse modeling has been demonstrated with the SCIAMACHY instrument on-board ENVISAT [*Bovensmann et al.*, 1999; *Frankenberg et al.*, 2005, 2008; *Bergamaschi et al.*, 2007; *Schneising et al.*, 2009]. However, its usefulness strongly depends on the precision and accuracy that can be achieved. Even systematic biases of less than 1% can compromise the usefulness of such measurements for inverse modeling if they are correlated on regional or seasonal scales [*Bergamaschi et al.*, 2007, 2009]. An important source of such errors are scattering events that take place along the light path

<sup>1</sup>Netherlands Institute for Space Research, Utrecht, Netherlands.

<sup>2</sup>IMK-ASF, Karlsruhe Institute of Technology, Eggenstein-Leopoldshafen, Germany.

<sup>3</sup>Jet Propulsion Laboratory, California Institute of Technology, Pasadena, California, USA.

<sup>4</sup>Institute of Environmental Physics, University of Bremen, Bremen, Germany.

<sup>5</sup>School of Chemistry, University of Wollongong, Wollongong, New South Wales, Australia.

<sup>6</sup>Arctic Research Center, Finnish Meteorological Institute, Helsinki, Finland.

<sup>7</sup>NIES, Tsukuba, Japan.

<sup>8</sup>National Institute of Water and Atmospheric Research, Wellington, New Zealand.

<sup>9</sup>IMK-IFU, Garmisch-Partenkirchen, Germany.

Corresponding author: D. Schepers, Netherlands Institute for Space Research, Sorbonnelaan 2, NL-3584 Utrecht CA, Netherlands. (d.schepers@sron.nl)

through the Earth's atmosphere [O'Brien and Rayner, 2002; Mao and Kawa, 2004; Houweling et al., 2005; Frankenberg et al., 2005; Aben et al., 2007]. Such scattering leads to a light path that differs from the straight line from sun to satellite observer through reflection at the Earth surface. The amount to which the light path is modified strongly depends on the micro-physical properties, height distribution and number density of the scattering particles as well as on the ground scene albedo. This makes properly accounting for light path modification when processing satellite measurements a major challenge.

[4] Currently, two conceptually different methods for retrieving CH<sub>4</sub> total column volume mixing ratio (VMR) are employed, differing in the way light path modification is treated. On the one hand the proxy retrieval aims to account for light path modification by simultaneously retrieving the total column of a proxy species, i.e. an atmospheric trace gas whose abundance in the atmosphere is assumed to be accurately known a priori. For CH<sub>4</sub> retrievals from SWIR measurements, CO<sub>2</sub> is the most suitable candidate [Frankenberg et al., 2005]. The retrieved CO<sub>2</sub> column serves as a light path proxy by comparing it to the prior knowledge. Differences between the two are assumed to be the result of light path modification, which is subsequently corrected for in the target gas retrieval. This method has been extensively used for methane retrievals from SCIAMACHY [Frankenberg et al., 2005, 2008; Bergamaschi et al., 2007; Schneising et al., 2009] and more recently it has been applied to methane retrievals from GOSAT [Parker et al., 2011]. On the other hand, so-called physics-based algorithms have been developed that aim to account for light path modification by modeling the scattering processes that underlie it. These algorithms retrieve information about atmospheric aerosols and (thin) clouds simultaneously with the methane column. Physics-based retrieval algorithms for CH<sub>4</sub> have recently been applied to synthetic and real GOSAT soundings [Butz et al., 2009, 2010; Bril et al., 2009; Butz et al., 2011].

[5] Butz et al. [2010] performed a comparison between proxy and physics-based methane retrievals using simulated GOSAT measurements for a realistic ensemble of atmospheric conditions. They concluded that overall the two methods perform comparably in accounting for the effect of atmospheric scattering, with slightly better performance by the proxy method. Proxy errors related to errors in the a priori CO<sub>2</sub> columns, a potentially important error source, were not investigated in the study of Butz et al. [2010]. In this paper, we compare both retrieval methods using true GOSAT measurements. Here, we perform validation of the two methods with ground based measurements of the Total Carbon Column Observing Network (TCCON). Additionally, we describe the results of two case studies that represent challenging scenarios concerning the atmospheric scattering properties and the a priori CO<sub>2</sub> fields. GOSAT measurements are discussed in section 2. For the proxy as well as the physics method we use a regularized least squares minimization. The retrieval concepts and specific setup of both retrievals algorithms are described in section 3. The two algorithms are verified by comparing corresponding GOSAT retrievals with collocated ground-based measurements and methane model

fields as presented in section 4. Conclusions are presented in section 5.

## 2. GOSAT Measurements

[6] GOSAT, launched on 23 January 2009, is the world's first dedicated satellite for measuring atmospheric concentrations of carbon dioxide and methane. It was placed in a Sun-synchronous orbit at an altitude of 666 km and crosses the equator around 1 p.m. local time with a three day revisit time. The instruments on-board GOSAT are a Fourier Transform Spectrometer (TANSO-FTS) and the Cloud and Aerosol Imager (TANSO-CAI) [Kuze et al., 2009].

[7] TANSO-FTS employs a Michelson interferometer to observe sunlight that is back-scattered or emitted by the Earth's surface and atmosphere in the SWIR and TIR spectral regions. The SWIR spectra are recorded in three separate bands between 0.758 and 2.08  $\mu\text{m}$  with a typical spectral resolution of about 0.3  $\text{cm}^{-1}$  [Kuze et al., 2009]. The TIR channel ranges from 5.56 to 14.3  $\mu\text{m}$ . TANSO-FTS has an instantaneous field of view of 15.8 mrad creating a footprint with approximately 5 km radius at sea level at the sub-satellite point. The instrument is capable of pointing  $\pm 35^\circ$  cross-track allowing it to take multiple cross-track soundings [Hamazaki et al., 2005]. During the time period covered by this research, TANSO-FTS was operated in 5 point mode (5 soundings cross-track) before 1 August 2010 and in three point mode after that date.

[8] The Cloud and Aerosol Imager (TANSO-CAI) consists of a radiometer with continuous spatial coverage with 1 km spatial resolution. It is used to retrieve cloud and aerosol properties, which allows for cloud filtering of TANSO-FTS soundings [Kuze et al., 2009].

[9] For this research the SWIR bands of TANSO-FTS are used to retrieve methane columns. In these bands, the back-scattered sunlight is recorded in two orthogonal polarization directions, from which the total back-scattered radiance signal is derived [Yoshida et al., 2011].

[10] For cloud screening, we implement a filter based on the TANSO-CAI L2 cloud flag data product. This product provides clear-sky confidence levels (from level 0, clear sky confidence less than 0.1, to level 15, clear sky confidence not less than 0.94) at  $\sim 1$  km spatial resolution at the sub-satellite point. We filter for clouded scenes by calculating the fraction of confidently clear-sky (level 15) TANSO-CAI pixels within a square box, centered at the TANSO-FTS footprint, with sides measuring approximately twice the TANSO-FTS footprint diameter. Considering a region considerably larger than the TANSO-FTS footprint minimizes the effect of spatial stray light which is scattered into the field of view by nearby clouds. A TANSO-FTS sounding is rejected if the fraction of confidently clear-sky TANSO-CAI pixels in the cloud screening box falls below 99% [Butz et al., 2011].

## 3. Retrieval Algorithm

### 3.1. Inversion

[11] The inversion algorithm aims to infer the state vector  $\mathbf{x}$  from a spectral observation  $\mathbf{y}$ . In this case the observation  $\mathbf{y}$  is defined as the observed spectrum of back-scattered SWIR

radiation measured by TANSO-FTS and the state vector  $\mathbf{x}$  contains the parameters to be retrieved. The observation  $\mathbf{y}$  and the state vector  $\mathbf{x}$  are related through a forward model  $\mathbf{F}$ :

$$\mathbf{y} = \mathbf{F}(\mathbf{x}, \mathbf{b}) + \epsilon. \quad (1)$$

Here, vector  $\mathbf{b}$  contains forward model parameters that are not retrieved, but must be known a priori. Furthermore,  $\epsilon$  denotes the combined contribution of measurement noise and forward model errors.

[12] The forward model  $\mathbf{F}$  is highly non linear in the state vector  $\mathbf{x}$ , so the problem of inverting equation (1) with respect to  $\mathbf{x}$  is solved in an iterative manner. For this, we propose the Gauss-Newton iteration scheme with reduced step size [Butz *et al.*, 2010], meaning that for iteration  $k$ , the forward model  $\mathbf{F}$  is linearized around the solution  $x_{k-1}$  of the previous iteration,

$$\mathbf{F}(\mathbf{x}, \mathbf{b}) = \mathbf{F}(\mathbf{x}_{k-1}, \mathbf{b}) + \mathbf{K}\Delta\mathbf{x} + \mathbf{O}(\Delta\mathbf{x}^2), \quad (2)$$

where  $\Delta\mathbf{x} = \mathbf{x} - \mathbf{x}_{k-1}$  and  $\mathbf{K}$  denotes the Jacobian matrix with elements defined as

$$K_{ij} = \frac{\partial F_i}{\partial x_j}(\mathbf{x}_{k-1}). \quad (3)$$

For each iteration step, equation (1) is inverted with respect to  $\mathbf{x}$  by minimizing a regularized least squares cost function, using the Phillips-Tikhonov regularization method [Phillips, 1962; Tikhonov, 1963]:

$$\tilde{\mathbf{x}}_k = \underset{\mathbf{x}}{\operatorname{argmin}} (\|\tilde{\mathbf{K}}\mathbf{x} - \tilde{\mathbf{y}}\|^2 + \gamma^2 \|\mathbf{x}\|^2). \quad (4)$$

with  $\tilde{\mathbf{y}} = \mathbf{S}_y^{-\frac{1}{2}}(\mathbf{y} - \mathbf{F}(\mathbf{x}_{k-1}, \mathbf{b}) + \mathbf{K}\mathbf{x}_{k-1})$  and  $\tilde{\mathbf{K}} = \mathbf{S}_y^{-\frac{1}{2}}\mathbf{K}$ . Here  $\mathbf{S}_y$  denotes the observation covariance matrix.

[13] The regularization is based on adding an extra term to the minimization that is sensitive to the propagation of measurement noise. The use of  $\mathbf{x}$  is appropriate in this case because methane is well mixed in the atmosphere and its vertical profile is smooth. Noise contributions on the retrieved state vector will increase the solution norm, thus making  $\mathbf{x}$  sensitive to noise propagation. Such regularization is introduced because a TANSO-FTS observation  $\mathbf{y}$  does not contain enough information to independently infer all retrieval parameters rendering the inverse problem ill-posed. Using an unregularized least squares approach would result in a solution that is overwhelmed by measurement noise that is associated with small singular values of the Jacobian  $\tilde{\mathbf{K}}$ . In equation (4) the regularization parameter  $\gamma$  is introduced to filter the contributions of these singular components from the solution  $\tilde{\mathbf{x}}_k$ . To illustrate this,  $\tilde{\mathbf{x}}_k$  can be written in terms of the singular value decomposition of  $\tilde{\mathbf{K}} = \mathbf{U}\Sigma\mathbf{V}^T$ :

$$\tilde{\mathbf{x}}_k = \sum_{i=1}^N \phi_i(\gamma) \frac{\mathbf{u}_i^T \tilde{\mathbf{y}}}{\sigma_i} \mathbf{v}_i, \quad (5)$$

where  $N$  is the dimension of state vector  $\mathbf{x}$ ,  $\mathbf{U}$  and  $\mathbf{V}$  are orthogonal matrices containing the left and right singular vectors  $\mathbf{u}_i$  and  $\mathbf{v}_i$  and  $\Sigma$  is a diagonal matrix containing the

singular values  $\sigma_i$ . The strictness of this filtering is governed by the regularization parameter  $\gamma$  through the filter factors

$$\phi_i(\gamma) = \frac{\sigma_i^2}{\sigma_i^2 + \gamma^2}. \quad (6)$$

To determine the optimal value of  $\gamma$  for each individual retrieval we use the L-curve method suggested by Hansen [1992]. The L-curve method enables us to regularize the retrieval based on the information content of the measurement, instead of regularizing based on prior knowledge as is done in the optimal estimation and related statistical regularization schemes. The regularized state vector can be written in terms of the true state vector  $\mathbf{x}_{true}$ :

$$\tilde{\mathbf{x}}_k = \mathbf{A}\mathbf{x}_{true} + \epsilon_x \quad (7)$$

Here,  $\epsilon_x$  denotes measurement noise and forward model errors that propagated onto the state vector. The averaging kernel matrix  $\mathbf{A}$  filters out those components of  $\mathbf{x}_{true}$  to which the measurement is insensitive. The formal definition of  $\mathbf{A}$  can be obtained by writing equation (5) in matrix form and substituting  $\tilde{\mathbf{y}} = \tilde{\mathbf{K}}\mathbf{x}_{true}$ :

$$\mathbf{A} = \mathbf{V}\Phi\mathbf{V}^T \quad (8)$$

with  $\Phi = \operatorname{diag}(\phi_i)$ .

[14] The components of  $\mathbf{x}_{true}$  to which the measurement is not sensitive are added to the solution state vector  $\hat{\mathbf{x}}$  from a prior estimate  $\mathbf{x}_a$ :

$$\hat{\mathbf{x}}_k = \tilde{\mathbf{x}}_k + (1 - \mathbf{A})\mathbf{x}_a. \quad (9)$$

### 3.2. Proxy Retrieval

[15] The proxy retrieval aims to account for light path modification by retrieving the total column of an atmospheric trace gas whose abundance in the atmosphere is assumed to be accurately known from prior sources [Frankenberg *et al.*, 2005]. The retrieved column serves as a light path proxy by comparing it to the prior knowledge. Differences between the two are assumed to be the result of light path modification, which is subsequently corrected for in the target gas retrieval. The assumptions underlying this retrieval method are that the light path modification in the spectral windows of the target and the proxy species is the same, as well as the relative vertical distribution of both species in the atmosphere. As proposed by Frankenberg *et al.* [2005] we use CO<sub>2</sub> as the light path proxy. Its atmospheric abundance is available from, for instance, the Carbon Tracker data assimilation system [Peters *et al.*, 2007] that is used in this research. For the retrieval, we use the R branch of the 2ν<sub>3</sub> methane band around 1.65 μm and the weakly absorbing CO<sub>2</sub> lines around 1.61 μm (windows 2 and 3 in Table 1). Figure 1 shows typical TANSO-FTS observations in these spectral windows. From the retrieved CH<sub>4</sub> and CO<sub>2</sub> profiles, the total column number densities [CH<sub>4</sub>] and [CO<sub>2</sub>] are readily calculated.

[16] Subsequently the column-averaged dry mole fraction of methane X<sub>CH<sub>4</sub></sub> is calculated through the following relation [Frankenberg *et al.*, 2005]:

$$X_{\text{CH}_4} = \frac{[\text{CH}_4]}{[\text{CO}_2]} \times X_{\text{CO}_2}. \quad (10)$$

**Table 1.** Spectral Range and Considered Absorbers for the Spectral Windows That are Used in the Proxy and Physics Retrieval Methods<sup>a</sup>

	Window Identification			
	1	2	3	4
Spectral range ( $\mu\text{m}$ )	0.758–0.774	1.591–1.622	1.629–1.654	2.042–2.081
Absorbers	O <sub>2</sub>	CO <sub>2</sub> H <sub>2</sub> O	CH <sub>4</sub> H <sub>2</sub> O, CO <sub>2</sub>	H <sub>2</sub> O, CO <sub>2</sub>
Physics	x	x	x	x
Proxy	-	x	x	-

<sup>a</sup>An 'x' indicates the windows that are used in the particular retrieval methods.

Here,  $X_{\text{CO}_2}$  is the total column dry mole mixing ratio of CO<sub>2</sub> from the CarbonTracker model. The use of [CO<sub>2</sub>] as the light path proxy in equation (10) implicitly assumes that neglect of scattering linearly scales the retrieved total columns of CH<sub>4</sub> and CO<sub>2</sub> to the same extent, such that it cancels out in the ratio [CH<sub>4</sub>]/[CO<sub>2</sub>]. Moreover, the accuracy of the CH<sub>4</sub> proxy retrieval is directly dependent on the accuracy to which the CO<sub>2</sub> concentrations can be modeled.

[17] For the proxy retrieval, the CO<sub>2</sub> and CH<sub>4</sub> column number densities are retrieved under the assumption of a

non-scattering atmosphere, thus assuming a direct light path from the Sun to the observing instrument in Earth orbit, via reflection at the Earth's surface. The state vector is formed by complementing the partial column number densities for CO<sub>2</sub> and CH<sub>4</sub> in 12 atmospheric layers, with the partial column number densities of interfering absorbers (see Table 1), the albedo of the ground scene and its spectral slope. The forward model parameter vector **b** contains pressure and temperature profiles and spectroscopic parameters which includes line-mixing for CO<sub>2</sub> and Oxygen

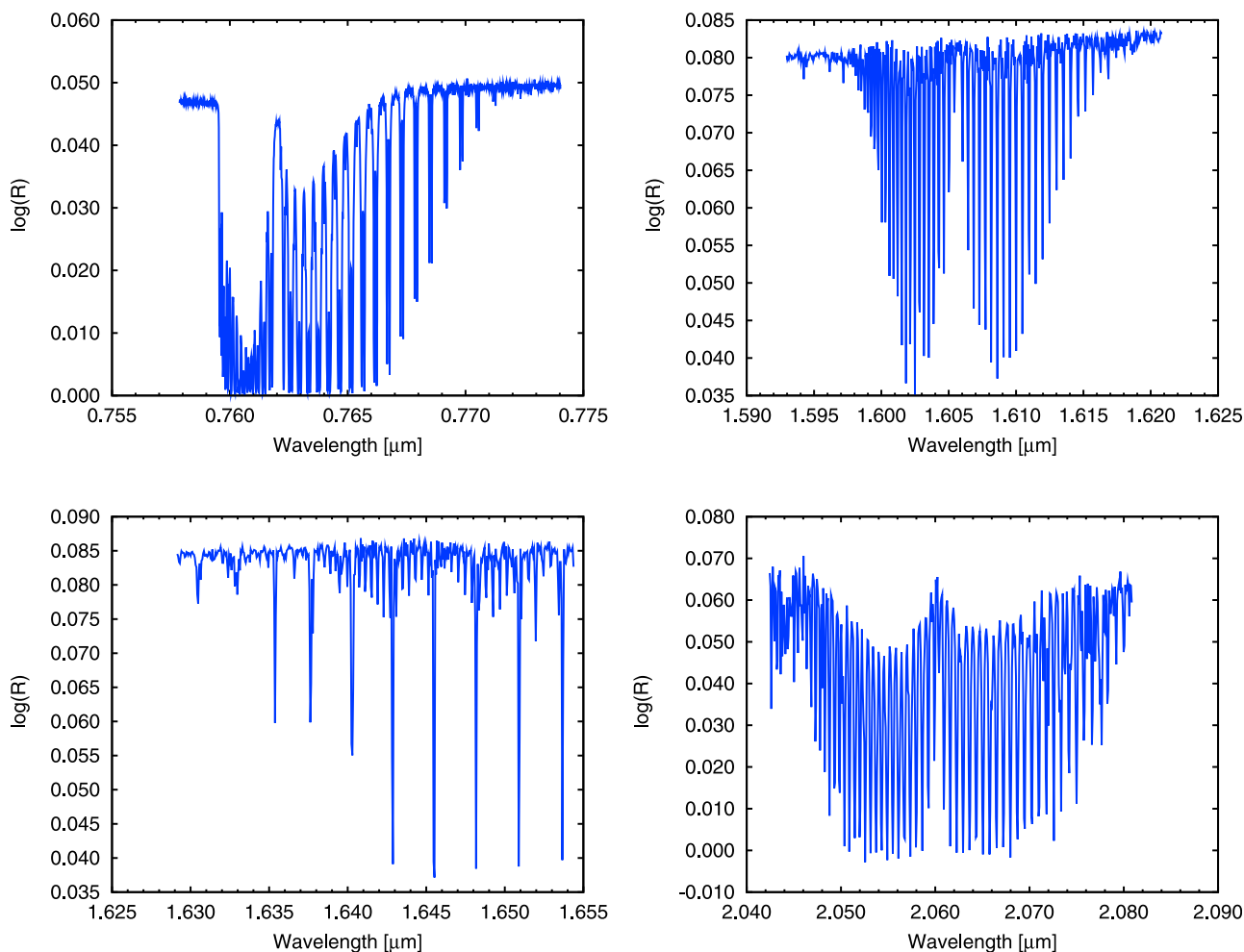


**Figure 1.** Typical TANSO-FTS reflectance measurements in the spectral windows that are used in the proxy and the physics retrieval: (top left) the O<sub>2</sub> A band, (top right) the weakly absorbing CO<sub>2</sub> lines around 1.6  $\mu\text{m}$ , (bottom left) the R-branch of the  $2\nu_3$  CH<sub>4</sub> band and (bottom right) the strongly absorbing CO<sub>2</sub> band around 2.0  $\mu\text{m}$ .

[Tran and Hartmann, 2008]. Profiles of atmospheric pressure, temperature and humidity that are used for our retrievals are provided by the ECMWF (European Center for Medium-Range Weather Forecast) ERA-interim analysis [Berrisford et al., 2009]. These data are provided 6-hourly on a 1.5 by 1.5 degree latitude/longitude grid and are interpolated onto the time and location of the TANSO-FTS observation. Surface elevation is extracted from the GTOPO30 digital elevation model. Initial guess profiles for methane are provided by a TM4 global transport model run for 2007 [Meirink et al., 2006]. The initial carbon dioxide profiles come from Carbon Tracker 2010 simulations [Peters et al., 2007] for the year 2009. Since CarbonTracker 2010 only provides CO<sub>2</sub> priors for 2009, we extrapolate the CO<sub>2</sub> model field to year 2010 which are required by our proxy retrieval. This extrapolation is done based on CO<sub>2</sub> background surface concentration measurements at three ground stations (Alert, Mauna-Loa and South Pole). For each month in 2010, an increase with respect to the same month in 2009 was determined and subsequently added to the global CarbonTracker CO<sub>2</sub> field.

[18] The proxy method has been extensively used for methane retrievals from SCIAMACHY near infrared soundings, for instance in Frankenberg et al. [2005, 2008]; Bergamaschi et al. [2007] and Schneising et al. [2009]. The main difference with our implementation is the inversion technique and the spectral windows that are used. Parker et al. [2011] employed a proxy retrieval method, using CO<sub>2</sub> as the proxy species, to retrieve methane total columns from TANSO-FTS SWIR measurements. In their setup a constant, fixed aerosol load was assumed in the forward model instead of the non-scattering atmosphere assumed in our setup. This disregards one advantage of the proxy method, namely the gain in computational speed that is realized by assuming a non-scattering atmosphere. Furthermore, where their inversion utilizes the optimal estimation method, we use Phillips-Tikhonov regularization to stabilize the retrieval.

### 3.3. Physics-Based Retrieval

[19] In contrast to the proxy method, the physics-based retrieval aims to deal with light path modification by explicitly modeling the atmospheric scattering processes that underlie it. The retrieval scheme utilizes the same Phillips-Tikhonov regularized inversion as the proxy method, but the retrieval setup is conceptually different. For the physics-based retrieval, the partial dry column number densities of methane are retrieved simultaneously with scattering properties of the model atmosphere. Subsequently, these number densities are converted to dry air total column mixing ratios using surface pressure data provided through the ECMWF's ERA-interim analysis [Berrisford et al., 2009]. The surface pressure is corrected to represent the dry air column using the humidity profile from the same ERA-interim analysis. This approach has been extensively discussed and applied to CO<sub>2</sub> and CH<sub>4</sub> retrievals from simulated measurements [Butz et al., 2009, 2010] and TANSO-FTS measurements [Butz et al., 2011]. The radiative transfer model developed by Hasekamp and Butz [2008] is employed in its scalar approximation mode, accounting for multiple scattering but neglecting polarization effects.

[20] Atmospheric scattering is described using a single aerosol layer parameterized by a Gaussian height distribution

and a power law size distribution. This parametrization is incorporated in the retrieval by adding three extra fit parameters to the state vector: the mean height of the aerosol layer, the size parameter of the power law distribution and an aerosol number density. The width of the aerosol layer is fixed to 2 km. The real and imaginary refractive indices are assumed wavelength independent and fixed to 1.4 and  $-0.003$  respectively. Butz et al. [2010] discuss the parametrization and the assumed characteristics of the modeled aerosol in a comprehensive manner. Note that by assuming a relatively simple aerosol model the retrieved aerosol parameters are effective scattering parameters that reproduce appropriate light path modification and thus might not be representative of the true properties of the aerosols within the TANSO-FTS field of view.

[21] The spectral observations used for the physics algorithm cover the methane and weak CO<sub>2</sub> absorption bands around 1.6  $\mu\text{m}$  that are also used in the proxy approach. To retrieve the effective scattering parameters, these bands are complemented with the strong CO<sub>2</sub> band around 2.0  $\mu\text{m}$  as well as with the oxygen A band at 760 nm (see Table 1). The additional two bands are modeled using a spectroscopy which includes line-mixing and collision-induced absorption in the oxygen A band. Typical observations in the spectral windows are shown in Figure 1.

## 4. Algorithm Verification

### 4.1. Validation With Ground-Based Measurements

[22] To validate our retrievals, we use methane and carbon dioxide column mixing ratio measurements provided through the Total Carbon Column Observing Network (TCCON) [Wunch et al., 2011]. The network uses ground-based sun-viewing Fourier Transform Spectrometer to obtain SWIR spectra, from which CH<sub>4</sub> and CO<sub>2</sub> column-average dry-air mole fractions can be retrieved. Based on aircraft overflights a global calibration factor is applied to the TCCON total column mixing ratios [Wunch et al., 2010].

[23] We selected 12 TCCON sites based on data coverage (both TCCON and GOSAT) and geographical location, such that they cover the largest possible latitudinal range. The selected TCCON sites are listed in Table 2 and their geographical locations are plotted in Figure 6. The TCCON site at Izana is excluded because all GOSAT soundings within the collocation criteria are located over the African mainland, where the surface elevation is  $\sim 2$  km lower than at Izana. This makes direct comparison of total columns difficult. For the remaining TCCON sites we consider 19 months of TANSO-FTS soundings between June 2009 and December 2010. Only GOSAT soundings within a 5° radius around the TCCON site are considered. After filtering for GOSAT error flags, soundings with a large solar zenith angle ( $>70^\circ$ ) or a large viewing angle ( $>30^\circ$ ) are discarded to prevent significant errors introduced both by the plane-parallel model atmosphere assumed in the forward model and by pointing instability associated with the TANSO-FTS instrument. Furthermore, soundings with highly variable surface elevation ( $>300$  m peak-to-peak) within the TANSO-FTS footprint and those with less than 99% confidently cloud free TANSO-CAI pixels in the cloud screening box (see section 2) are not considered to prevent errors through topography or (partial) cloud cover.

**Table 2.** Latitude, Total Number of TCCON-GOSAT Retrieval Pairs (N), Average Albedo, the Average Retrieval Bias (b) (TCCON - GOSAT) and the Single-Sounding Precision ( $\sigma$ ) of the GOSAT X<sub>CH<sub>4</sub></sub> Retrievals at the Selected TCCON Stations Using the Physics and Proxy Retrieval Methods<sup>a</sup>

Station Number	Station	Latitude (deg)	N	Albedo at 1.6 $\mu\text{m}$	Physics		Proxy	
					$\sigma$ (ppb)	b (%)	$\sigma$ (ppb)	b (%)
1	Sodankyla	67.37	37	0.144	17	-0.836	22	-0.312
2	Bialystok	53.23	138	0.180	16	-0.324	17	0.306
3	Bremen	53.10	88	0.182	14	-0.385	17	0.122
4	Karlsruhe	49.10	110	0.185	18	-0.492	20	-0.157
5	Orleans	47.97	199	0.197	13	-0.314	16	0.173
6	Garmisch	47.48	149	0.184	19	-0.081	19	0.421
7	Park Falls	45.95	338	0.188	16	-0.429	16	-0.104
8	Lamont	36.60	1315	0.252	15	-0.379	15	0.040
9	Tsukuba	36.05	14	0.156	19	-0.070	14	0.333
10	Darwin	-12.43	91	0.254	13	-0.498	9	-0.045
11	Wollongong	-34.41	131	0.245	20	-0.286	16	0.145
12	Lauder	-45.05	18	0.270	20	-0.816	16	-0.121
All stations			2628		$\bar{\sigma} = 17$ $\sigma_{bias} = 0.24$	$\bar{b} = -0.37$	$\bar{\sigma} = 17$ $\sigma_{bias} = 0.22$	$\bar{b} = 0.06$

<sup>a</sup>At the bottom of the table the mean bias  $\bar{b}$ , the mean single sounding precision  $\bar{\sigma}$  and the standard deviation of the station biases ( $\sigma_{bias}$ ) is given for each retrieval method.

[24] The resulting set of soundings was processed with both the physics and proxy algorithms. Subsequently the results were filtered based on the spectral fit, discarding soundings with a  $\chi^2 > 4$ . In addition, scenes with significant cirrus contamination are filtered out using a filter based on the radiance level in the strongly absorbing water bands in the 2  $\mu\text{m}$  region. The possibility of applying an a posteriori filter based on the retrieved effective scattering parameters is unique to the physics retrieval method. Such filter was proposed by Butz *et al.* [2010], discarding all cases for which  $\omega_s \equiv \tau_s \times 1/\alpha_s \times z_s$  is larger than a threshold value  $\omega_{max}$  that governs the strictness of the filter. Here  $\tau_s$ ,  $\alpha_s$  and  $z_s$  denote the aerosol optical thickness, the power law size parameter and height of the aerosol layer that are fitted in the physics retrieval. In other words, a sounding is most likely discarded in case of optically thick aerosol and cirrus with large scattering particles high in the atmosphere. Butz *et al.* [2010] applied a threshold of  $\omega_{max} = 300$  m, which has been empirically determined. Unless stated otherwise, this filter has been applied to the physics retrieval results presented here.

[25] To compare similar data sets, the proxy results are also filtered such that only soundings are considered that passed the posterior aerosol filter in the physics retrieval. Figures 2 and 3 show resulting X<sub>CH<sub>4</sub></sub> time series over the selected TCCON sites. In the same panel, all TCCON X<sub>CH<sub>4</sub></sub> values retrieved within  $\pm 2$  hours of the GOSAT overpass time are plotted.

[26] At first glance, both the physics and the proxy algorithms reproduce the (seasonal) variation of X<sub>CH<sub>4</sub></sub> that is present in the ground-based data equally well, while the proxy retrievals show consistently higher mixing ratios than the physics retrievals. Also, it shows that GOSAT data coverage over the TCCON sites has a strong seasonal dependence resulting, for instance, in a data gap in winter for most of the northern hemisphere stations.

[27] For a quantitative comparison of our retrievals we define the mean of the difference between collocated GOSAT-TCCON retrieval pairs as the retrieval bias  $b$ . The standard deviation  $\sigma$  of the differences is used to estimate the

single-sounding precision of our retrievals. We use the standard deviation of the station biases  $\sigma_{bias}$  to estimate the inter station bias variability. Furthermore we define the mean retrieval bias  $\bar{b}$  by averaging all station biases weighted by the number of soundings per station. Similarly, the mean single sounding precision  $\bar{\sigma}$  is obtained by taking the weighted average of the estimated single sounding precisions for each station.

[28] Table 2 shows the bias  $b$  and the estimated single-sounding precision  $\sigma$  for each of the TCCON sites as well as the number of data points  $N$  used for the analysis. For the physics retrieval method the bias ranges from -0.836% at Sodankyla to -0.081% at Garmisch with a standard deviation of 0.24% and a single sounding precision typically between 13 and 20 ppb. For the proxy retrievals we find station-dependent biases that range from -0.312% at Sodankyla to 0.421 at Garmisch, with a 0.22% standard deviation and a single sounding precisions between 9 ppb and 21 ppb. Based on the presented comparison at the 12 TCCON validation sites, both retrievals shows very similar performance in terms of station to station bias variability  $\sigma_{bias}$ .

[29] The difference in terms of bias with respect to TCCON between the physics retrievals ( $\bar{b} = -0.37$ ) and the proxy retrievals ( $\bar{b} = 0.06$ ) could be caused by the fact that the physics retrieval employs two spectral bands that are not used in the proxy approach, which might introduce a bias through spectroscopy. In the proxy retrievals, radiometric calibration inaccuracies are likely to cancel out as it takes the ratio of retrieved [CH<sub>4</sub>] and [CO<sub>2</sub>] columns, however spectroscopic errors might introduce inconsistency between retrieved CO<sub>2</sub> column and the prior CO<sub>2</sub> column, potentially leading to a bias in X<sub>CH<sub>4</sub></sub> (see equation (10)).

[30] For an overall evaluation of the different retrieval approaches based on the presented results, one should keep in mind several aspects. The difference, in terms of inter station bias variability  $\sigma_{bias}$ , between the proxy and the physics retrievals is small which makes it difficult to judge the significance of these results. Second, the present TCCON sites are limited for validation purposes for several

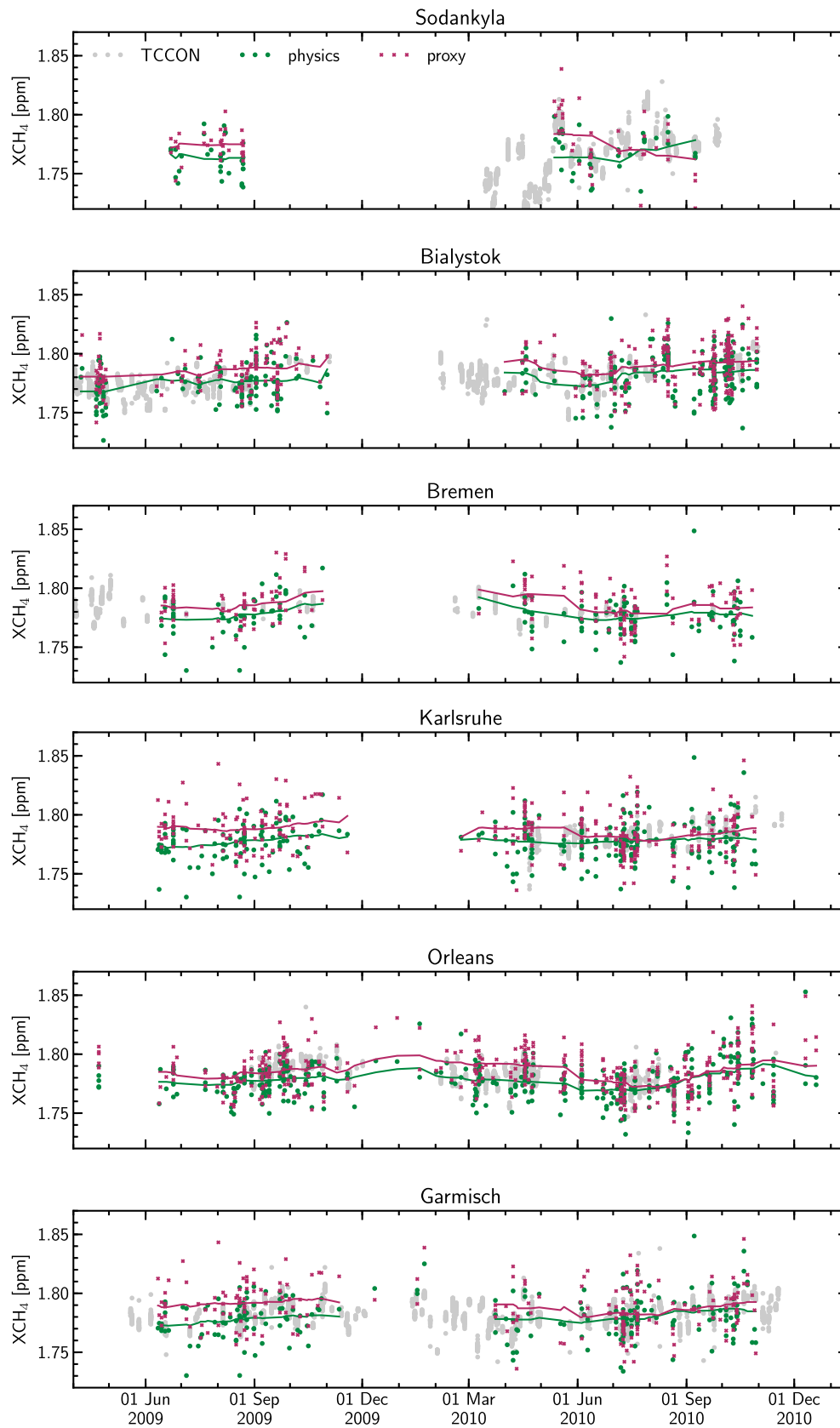


**Figure 2.** Time series of  $X_{\text{CH}_4}$  over selected TCCON stations. Ground-based-FTS retrievals from TCCON (gray) are overplotted with our TANSO-FTS retrievals using the physics algorithm (green dots) and the proxy algorithm (red crosses). The lines represent smoothed time series using a 10-day boxcar running mean. All TCCON retrievals within  $\pm 2$  hours of a GOSAT overpass are plotted.

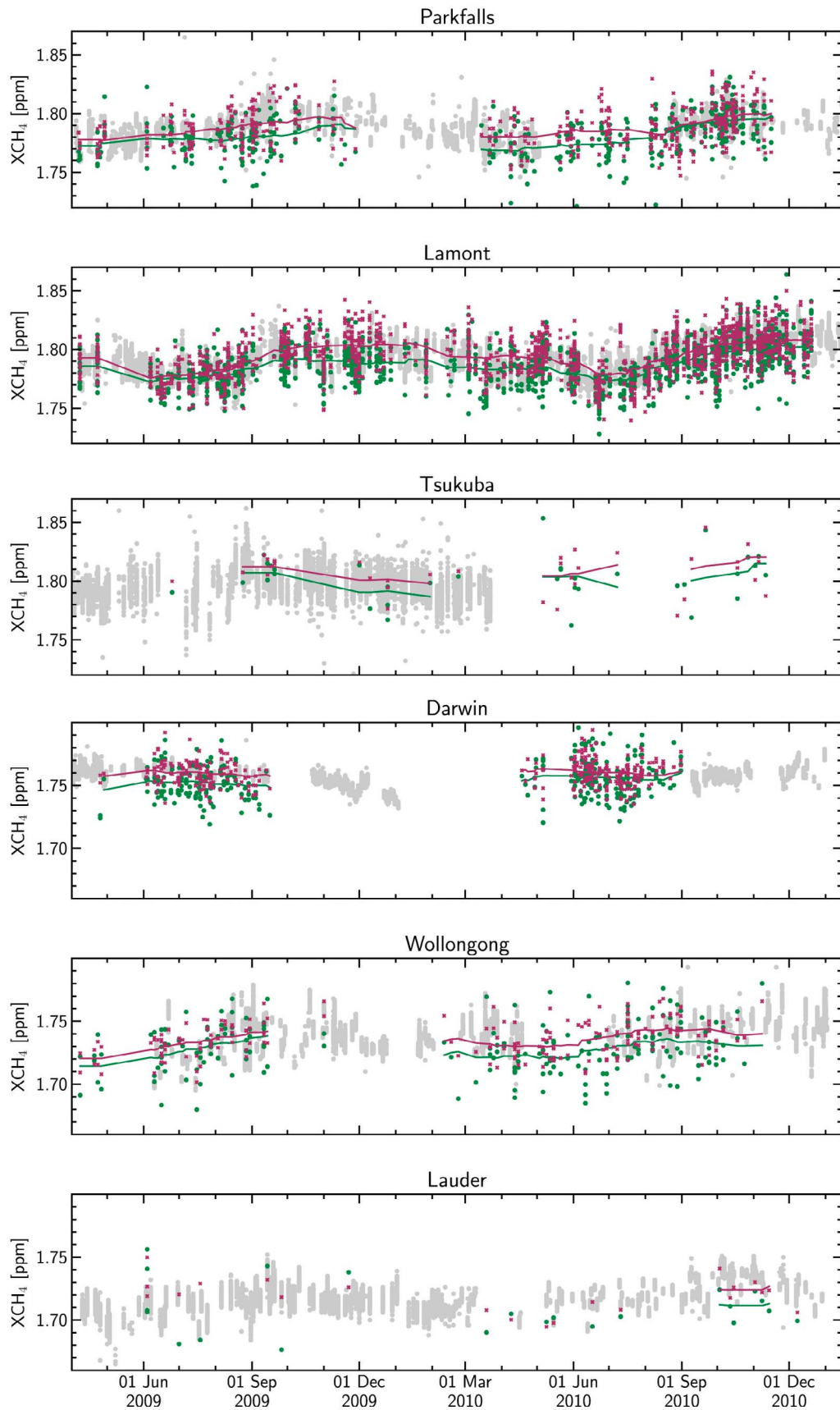


**Figure 3.** Same as Figure 2, for additional locations.



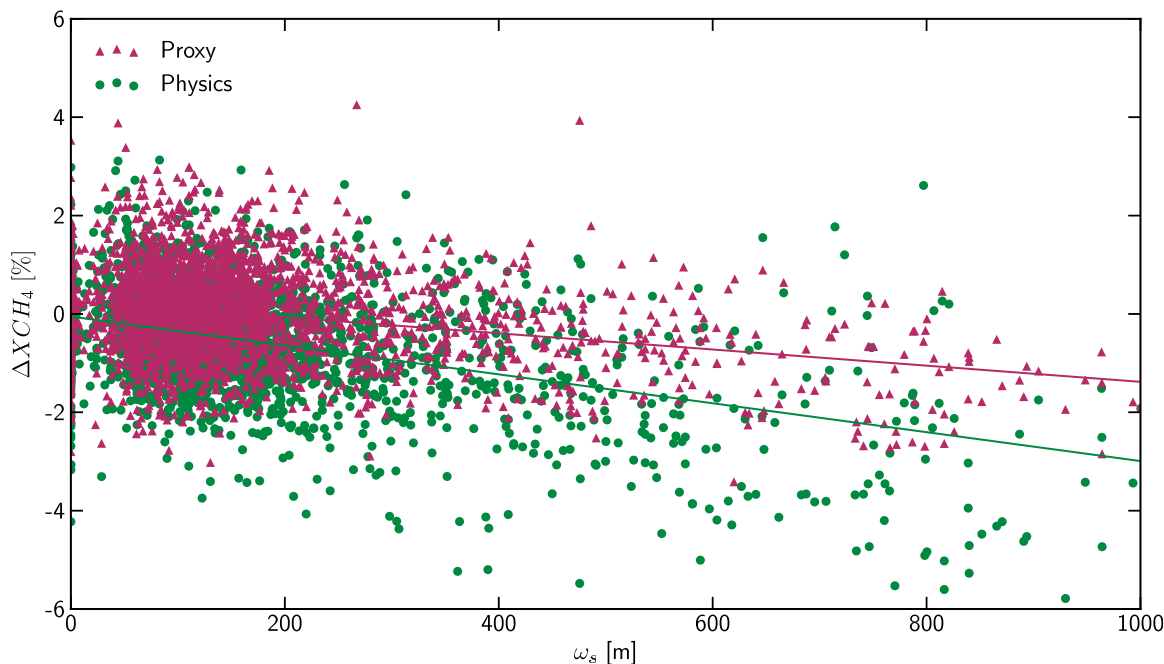


**Figure 4.** Retrieval residuals (GOSAT-TCCON) over all considered TCCON sites for proxy and physics retrievals as function of the scattering parameter  $\omega_s$ . Linear regression lines are drawn through both point clouds.

reasons. Apart from a limited spatial coverage, the TCCON sites used in this study show a very limited range in ground scene albedo (average albedo in Table 2 varies between 0.144 and 0.270 where the full range around 1.6  $\mu\text{m}$  covers  $\sim 0.05$ – $0.75$  (P. Tol, personal communication, 2010) [Butz *et al.*, 2010]) and most of the stations suffer from seasonal data gaps in both TCCON and GOSAT data, mostly caused by the presence of clouds or instrument issues. Thirdly, in order to create two comparable sets of soundings, the proxy data have been filtered strictly by only considering those soundings that passed posterior filtering based on the physics retrieval. This may hide any advantage or disadvantage of the proxy method. Overall, these aspects make it hard to draw conclusions on the overall performance of both retrieval approaches. To gain more insight into this we investigate the effect of seasonal data coverage and the posterior scattering filter more in-depth.

[31] The posterior scattering filter is unique to the physics approach. Applying it to the proxy results was only necessary to create equal data sets. We investigate how such filtering influences the retrieved  $X_{\text{CH}_4}$  for both retrieval methods. Figure 4 shows the residual methane total columns from individual GOSAT retrievals with respect to collocated TCCON measurements, as a function of the scattering filter quantity  $\omega_s$ . As expected, the physics retrieval residuals show a clear dependence on  $\omega_s$ , underestimating  $X_{\text{CH}_4}$  by more than 4% for  $\omega_s > 300$  m. This indicates that the physics approach has limited effectiveness when dealing with many scattering particles located high up in the atmosphere and also represents the main motivation for introducing the filter with  $\omega_{\text{max}} = 300$  m. The proxy retrievals also show a clear dependence on atmospheric scattering properties. Although this dependence is smaller than for the physics retrieval it

leads to a maximum underestimation of  $X_{\text{CH}_4}$  by  $>1\%$  for high values of  $\omega_s$  for the proxy method. This dependence on atmospheric scattering can be traced back to the ratio term  $[\text{CH}_4]/[\text{CO}_2]$ . We did not expect this behavior since the effects of scattering in the atmosphere are assumed to cancel out by taking the ratio. Thus, in order to achieve an overall accuracy of  $<1\%$ , the proxy retrieval also needs some a posteriori filtering, although it can be significantly relaxed with respect to the a posteriori filtering applied in this study. It is however important to note that the filter we have applied is based on retrieval parameters that are only available when using the physics retrieval approach.

[32] Continuous data coverage throughout the year at the TCCON site at Lamont enables us to compare the seasonal cycles that are retrieved by both retrieval methods. Figure 5 shows the residuals in percent of the total column mixing ratio for individual proxy and physics retrievals with respect to collocated TCCON measurements. Here, the annual mean difference has been subtracted for both retrievals. The proxy retrievals clearly show a temporal variation of the residuals with an amplitude of  $\sim 0.75\%$  of the total column mixing ratio. Between September 2009 and May 2010, the proxy retrieval overestimates the TCCON methane columns, while it underestimates TCCON methane columns from June to December 2010. The proxy residuals can subsequently be split into contributions of the ratio term  $[\text{CH}_4]/[\text{CO}_2]$ , and the CarbonTracker prior  $\text{CO}_2$  column (see equation (10)) by comparing these quantities to ground based measurements independently. In the same panel, the residuals of the ratio term and the a priori  $\text{CO}_2$  column with respect to TCCON measurements are also plotted. Clearly, the proxy retrieval residuals over the Lamont site predominantly stem from the residuals in the ratio term, indicating that uncertainties in the

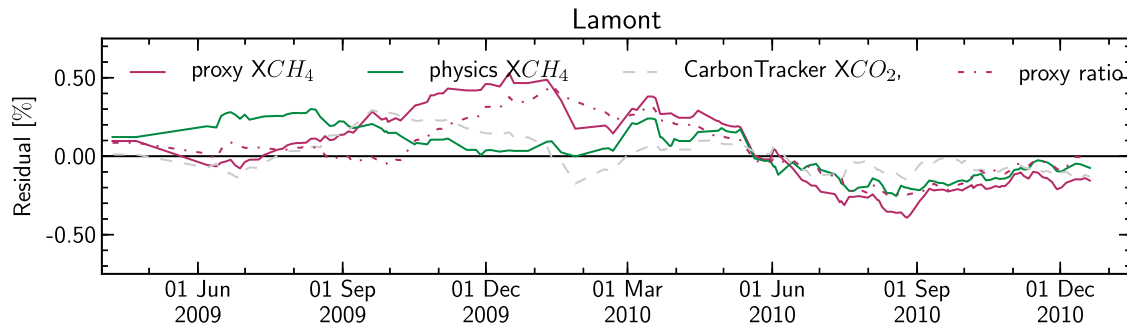


**Figure 5.** Residual seasonal cycles at Lamont (GOSAT - TCCON) for proxy and physics retrievals. Also the residuals of the proxy ratio  $[\text{CH}_4]/[\text{CO}_2]$  and CarbonTracker prior  $\text{CO}_2$  with respect to TCCON ground-based measurements are plotted. The time series is smoothed using a 10-day boxcar running mean, and the annual mean difference has been subtracted.

$\text{CH}_4$  and  $\text{CO}_2$  column density retrievals do not always cancel out to the same extent by taking their ratio. The temporal variation of the residuals on the ratio term seems to indicate some seasonal dependence, however the short data record and significant differences between behavior in 2009 and 2010 make it hard to conclude on that with certainty at this point. Note that due to the seasonal data gaps at the majority of the TCCON sites, the values in Table 2 are biased towards the summer season.

[33] Butz *et al.* [2010] discuss the following three potential error sources in the proxy ratio as a result of atmospheric scattering: (1) differences in the optical properties of the scattering particles and molecules in the  $\text{CH}_4$  and  $\text{CO}_2$  retrieval ranges, (2) difference in surface albedo between the  $\text{CH}_4$  and the  $\text{CO}_2$  retrieval windows and (3) differing height sensitivities of the  $\text{CH}_4$  and  $\text{CO}_2$  retrievals. For synthetic measurements, the second and third error source were found to be both in the 0.5% range with opposite sign leading to a cancelation of errors in many cases. Therefore, a likely explanation for the time dependent bias of the proxy retrievals could be found in variation of these two error sources: Assuming two error sources of similar magnitude and opposing sign show different variations in time, the net result would be a retrieval bias that varies in time.

#### 4.2. Scenarios Not Covered by Ground-Based Measurements

[34] In this section we compare our retrievals with model calculations using a global multiyear model assimilation of methane abundances considering two regions of the globe that show considerable differences between proxy and physics retrievals and are not covered by the validation with TCCON ground-based measurements. Both regions are indicated in Figure 6. The methane model fields are assimilated for the period 2009–2010 using *in situ* measurements provided through the Earth System Research Laboratory (ESRL) global air sampling network [e.g., Dlugokencky *et al.*, 2009]. The assimilation scheme [Meirink *et al.*, 2008a, 2008b] is driven by the atmospheric transport model TM5 [Krol *et al.*, 2005] on a  $4^\circ \times 6^\circ$  (latitude  $\times$  longitude) grid. For each GOSAT sounding, processed with both our retrieval algorithms, that passed filtering with  $\omega_{\text{max}} = 300$  m, a collocated  $X_{\text{CH}_4}$  profile is extracted from the TM5-NOAA optimized fields and integrated to a methane total column mixing ratio. In this way, three data sets are created that can be directly compared.

[35] We observe prominent differences between our proxy and physics retrievals over the Sahara. Time series of retrieved  $X_{\text{CH}_4}$  over this region are shown in Figure 7. In the

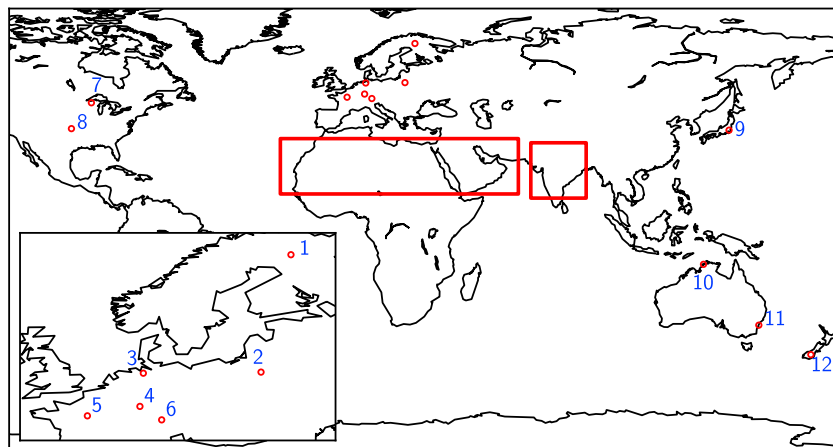


**Figure 6.** Regions of the globe that we selected to compare our retrievals against TM5-NOAA methane fields: the Sahara and Arabian peninsula and the Indian subcontinent. The locations of the TCCON stations used in this research are indicated and numbered according to Table 2.

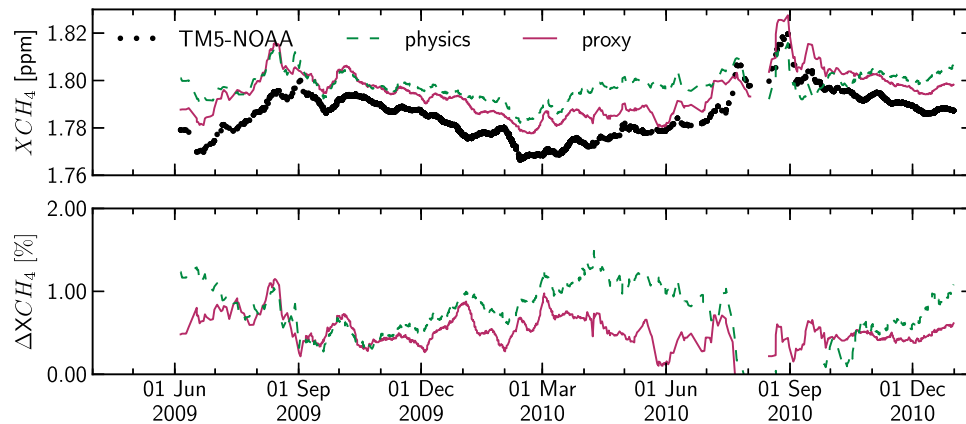


**Figure 7.** (top) Time series of  $X_{\text{CH}_4}$  retrieved with the proxy method and the physics method as well as  $X_{\text{CH}_4}$  from the TM5-NOAA inversion over the Sahara region. (bottom) Time series  $X_{\text{CH}_4}$  residuals (GOSAT - TM5-NOAA) over the Sahara region. Both time series are smoothed with a 10 day boxcar running averaging function.

same figure, the time series of collocated  $X_{\text{CH}_4}$  model results are plotted. The latter are off-set by the global average difference between the physics retrievals and TM5-NOAA. We find that the physics method consistently retrieves higher  $X_{\text{CH}_4}$  than the proxy method during spring and summer, while in winter both methods agree. Overall, the seasonal cycle of the proxy retrieval agrees better with TM5-NOAA than the physics retrievals. The difference in spring and summer coincides with increased dust storms in the Sahara region, resulting in high scattering optical thickness. This is illustrated in Figure 8 where the residuals  $\Delta X_{\text{CH}_4}$  between the retrieved and modeled  $\text{CH}_4$  column densities are plotted as a function of collocated aerosol optical depth at  $0.66 \mu\text{m}$  as seen by MODIS Terra [Remer *et al.*, 2005] for the Sahara region. Here, aerosol optical depth is correlated with an

overestimation of methane total column by the physics method, even when the a posteriori scattering filter has been applied. This behavior is comparable, although smaller in magnitude, to the behavior of non-scattering retrievals in the presence of aerosol [Aben *et al.*, 2007], which indicates that the physics retrieval does not sufficiently account for scattering in high optical depth scenes over bright surfaces. Also the proxy retrieval shows this behavior but to a lesser extent, once more indicating that not all uncertainties introduced by scattering cancel out by taking the ratio  $[\text{CH}_4]/[\text{CO}_2]$ .

[36] To indicate the significance of this dependence on MODIS optical thickness, we estimated the uncertainty on the slope of the linear regression using the spread of the data around their regression as an overall estimate for data

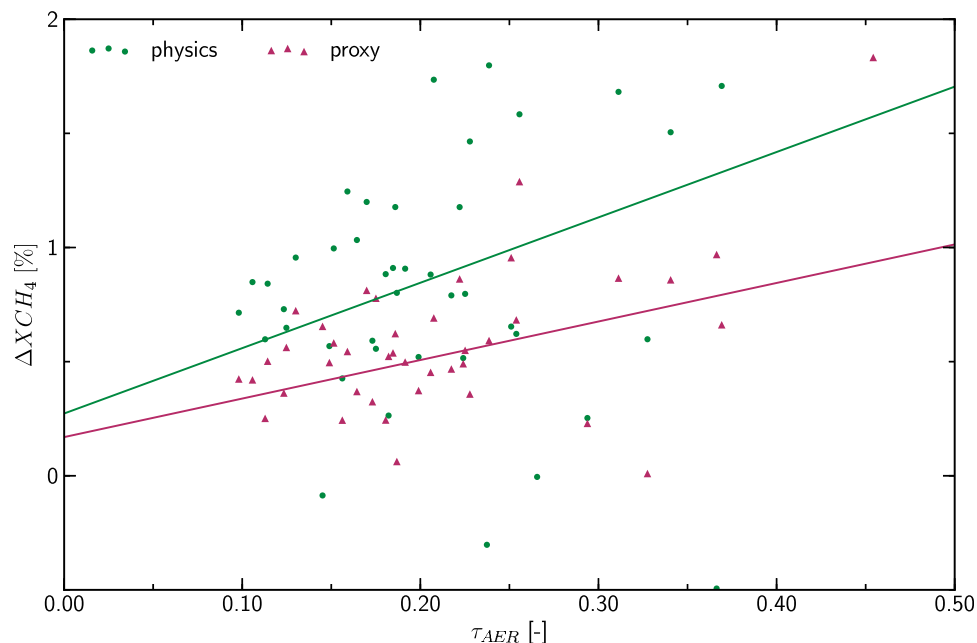


**Figure 8.** Retrieval residuals (GOSAT - TM5-NOAA) as function of collocated MODIS optical depth at  $0.66 \mu\text{m}$  over the Sahara region [Remer *et al.*, 2005]. The data points were obtained using a 10 day box-car average. Linear regression lines are drawn through both point clouds.

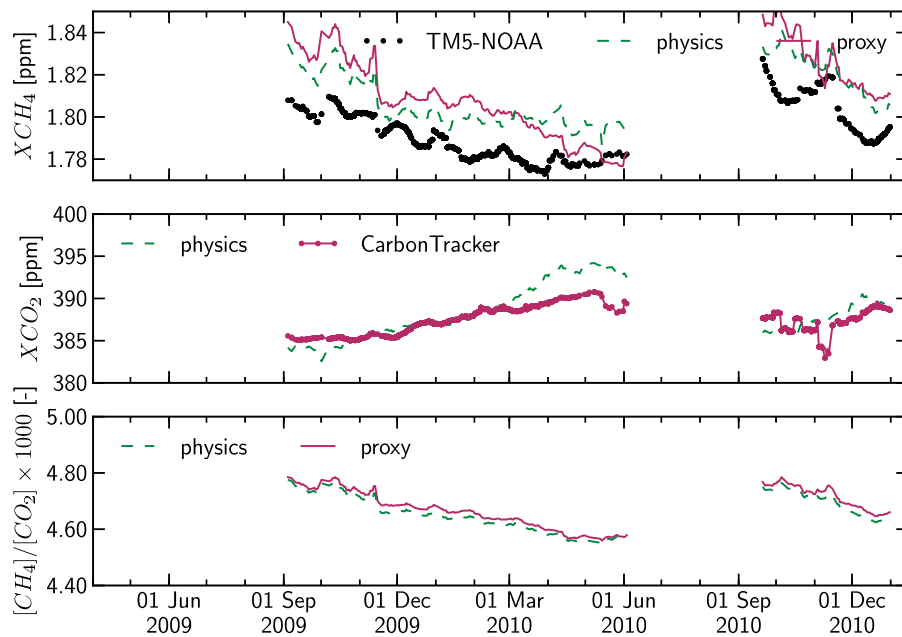


**Figure 9.** (top) Time series of  $X_{\text{CH}_4}$  retrieved with the proxy method and the physics method as well as  $X_{\text{CH}_4}$  from the TM5-NOAA inversion over the Indian subcontinent. (middle) Time series of  $X_{\text{CO}_2}$  retrieved with the physics method and the prior  $X_{\text{CO}_2}$  from CarbonTracker that is used for the proxy retrievals. (bottom) The ratio  $[\text{CH}_4]/[\text{CO}_2]$  used in the proxy retrieval compared to  $X_{\text{CH}_4}/X_{\text{CO}_2}$  retrieved by the physics method. All time series are smoothed using a 10-day boxcar running mean.

uncertainty. In both cases, the one sigma uncertainty is similar in value to the slope of the regression line, leading us to conclude that the dependence can be detected with a one sigma confidence.

[37] Analogous to the discussion of performance over desert areas, we investigate the retrieval performance over

the Indian subcontinent. Time series of retrieved and modeled  $X_{\text{CH}_4}$  over this region are plotted in Figure 9 (top) which shows that the proxy retrieval gives a seasonal cycle with a larger amplitude than the physics retrieval and the TM5-NOAA inversion. This effect is most prominent in spring, when the proxy retrieval shows a continuous decrease in

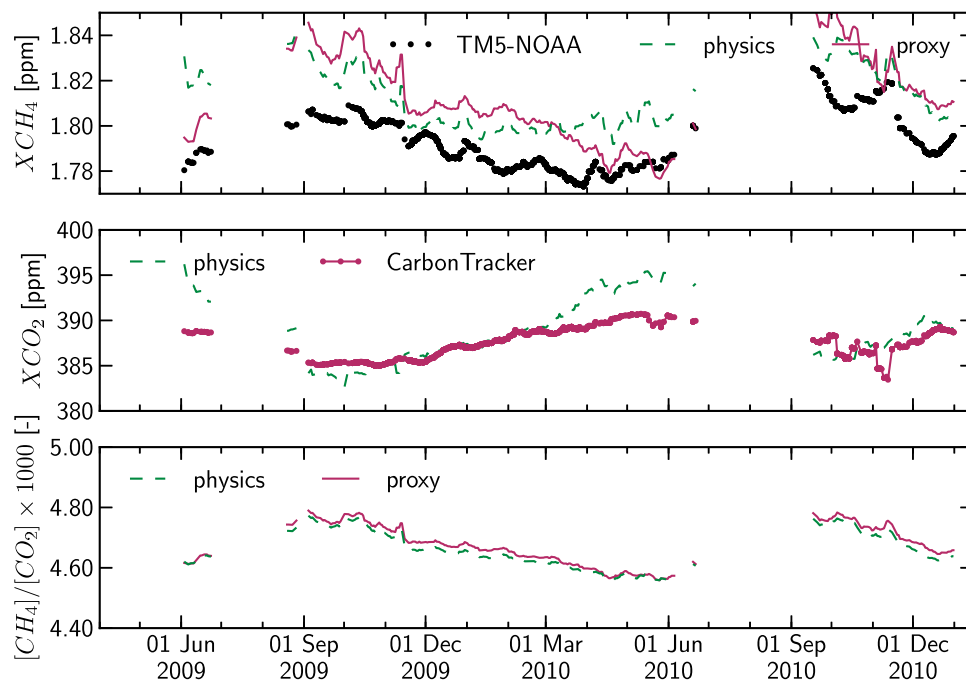


**Figure 10.** Same as Figure 9 but without the posterior aerosol filter applied to retain more data in summer 2009.

$X_{\text{CH}_4}$  while the physics retrievals and TM5-NOAA show a virtually constant methane column mixing ratio. We identified the source of this feature by comparing the proxy ratio and the CarbonTracker prior CO<sub>2</sub> against  $X_{\text{CH}_4}/X_{\text{CO}_2}$  and  $X_{\text{CO}_2}$  from the physics retrieval. Figure 9 (middle and bottom) show that the underestimation of methane by the proxy method in spring coincides with a period in which the CarbonTracker CO<sub>2</sub> fields underestimate the physics CO<sub>2</sub> retrievals. The fact that  $X_{\text{CH}_4}$  from the physics retrieval follows the seasonality of TM5-NOAA combined with agreement between  $[\text{CH}_4]/[\text{CO}_2]$  and the  $X_{\text{CH}_4}/X_{\text{CO}_2}$  ratio from the physics retrieval gives us confidence in the latter. To rule out the possibility that this feature is a consequence of the extrapolation of CarbonTracker 2009 fields to 2010, Figure 10 shows the same data sets but without the posterior scattering filter applied. By dropping the filter we gain enough data in June 2009 to see the same feature as we see in spring 2010; i.e. the proxy method retrieves lower values of  $X_{\text{CH}_4}$  than the physics retrieval, while CarbonTracker shows lower total column CO<sub>2</sub> mixing ratios than the physics retrieval. This leads us to conclude that an erroneous seasonal cycle (amplitude) in CarbonTracker introduces significant errors in methane column mixing ratios retrieved by the proxy method over the Indian subcontinent where CarbonTracker is poorly constrained [Patra *et al.*, 2011].

[38] In summary, the results of our study agree with results from the study by Butz *et al.* [2010] based on synthetic GOSAT measurements. Butz *et al.* [2010] concluded that both the physics as well as the proxy retrievals are capable of retrieving  $X_{\text{CH}_4}$  in aerosol loaded scenes with retrieval errors less than 1%, which agrees with our findings. In accordance with that same study, we also find that the proxy retrieval shows a more narrow distribution of errors than the physics retrievals, where the latter benefits from filtering scenes containing elevated layers of coarse aerosol. Furthermore, using real GOSAT measurements, we confirmed the statement made by Butz *et al.* [2010] that the proxy retrieval errors are likely to be dominated by errors in the prior  $X_{\text{CO}_2}$ .

## 5. Conclusions

[39] We presented a performance analysis comparing two algorithms for retrieving methane total column mixing ratios from GOSAT measurements of back-scattered shortwave infrared solar radiation. The algorithms differ in the way they treat the effect of scattering by aerosols and cirrus particles on the retrieved methane column density. On the one hand, the proxy method relies on retrieving CO<sub>2</sub> as a proxy for light path. On the other hand, the physics algorithm aims to model any light path modification using three effective retrieval parameters that govern the model atmosphere's scattering properties.

[40] A comparison of these algorithms with ground-based measurements of CH<sub>4</sub> total column was carried out at 12 TCCON stations around the globe. Using a 19 month data set, ranging from June 2009 to December 2010, we find that both retrievals perform very similarly in terms of inter-station bias and precision. For the proxy retrieval we find a station averaged retrieval bias with respect to ground-based measurements that varies from  $-0.312\%$  to  $0.421\%$  with a standard deviation of  $0.22\%$  and a typical precision of 17 ppb. For the physics retrieval we find biases between  $-0.836\%$

and  $-0.081\%$  with a standard deviation of  $0.24\%$  and a typical precision of 17 ppb. At the TCCON site at Lamont, where there is data coverage throughout the year, we find that residuals of the proxy retrieval show a temporal dependence of  $\sim 1\%$  peak-to-peak. For the physics retrievals this peak-to-peak variation amounts to  $\sim 0.5\%$ . For both retrievals we find that the residuals with respect to TCCON measurements show a dependence on the amount of scattering. For the physics algorithm this amounts to a maximum underestimation of  $\sim 4\%$  when no filter is applied to reject highly scattering scenes. Surprisingly, the proxy retrievals also show a clear dependence on atmospheric scattering, amounting to  $>1\%$  of the total column. This behavior is unexpected because scattering effects are assumed to cancel out in the proxy method. Thus, in order to achieve an overall retrieval accuracy of  $<1\%$  both retrievals need some form of a posteriori filtering. This analysis, based on comparison with ground-based measurements, cannot be considered to be fully representative for global retrievals because of the limited spatial coverage, the small albedo range and the seasonal data gaps at many TCCON stations. To complement the validation with ground-based measurements, we compared both retrievals with simulated methane fields from a global multiyear inverse data scheme, assimilating in situ ground-based measurements of methane.

[41] We found a pronounced difference between the different retrievals over the desert regions of North Africa and the Middle East, where the physics retrieval overestimated total column CH<sub>4</sub> by  $\sim 1\%$  in the high aerosol optical depth atmosphere. This indicates that scattering over bright surfaces is not treated properly by the physics method.

[42] Over the Indian subcontinent the proxy retrieval overestimates the amplitude of the seasonal cycle, especially overestimating CH<sub>4</sub> mixing ratios by up to 1% in spring. This feature was traced back to an erroneous seasonal cycle amplitude in the prior CO<sub>2</sub> fields used to determine light path modification.

[43] Overall, the results of our study agree with results from the study by Butz *et al.* [2010] based on synthetic GOSAT measurements. Using real GOSAT measurements, we confirmed that both the proxy and the physics method are capable of retrieving  $X_{\text{CH}_4}$  in aerosol loaded scenes with retrieval errors less than 1%, where the physics method strongly benefits from filtering scenes containing elevated layers of coarse aerosol. Furthermore we confirmed that the retrieval errors of the proxy method are likely to be dominated by errors in the prior  $X_{\text{CO}_2}$ .

[44] Although the relevance of these findings for an overall analysis of retrieval performance is hard to estimate, we did identify some typical weaknesses in both retrieval approaches. Furthermore, our results indicate that the limited spatial and albedo coverage of the present sites within the TCCON limits its suitability for validation of methane retrievals from satellite measurements. We believe that extending the network of validation stations is essential for gaining more insight in the performance of methane total column retrieval from space-borne shortwave infrared measurements.

[45] **Acknowledgments.** A.B. is supported by Deutsche Forschungsgemeinschaft (DFG) through the Emmy-Noether programme, grant BU2599/1-1 (RemoteC). Access to GOSAT data was granted through the 2nd GOSAT research announcement jointly issued by JAXA,

NIES, and MOE. TCCON data were obtained from the TCCON Data Archive, operated by the California Institute of Technology from the Web site at <http://tcon.ipac.caltech.edu/>. GTOPO30 is available from the U.S. Geological Survey through the Earth Resources Observation and Science (EROS) Center ([http://eros.usgs.gov/#/Find\\_Data/Products\\_and\\_Data\\_Available/GTOPO30\\_info](http://eros.usgs.gov/#/Find_Data/Products_and_Data_Available/GTOPO30_info)). MODIS Atmosphere data are distributed through <http://ladsweb.nascom.nasa.gov/data/search.html>. CarbonTracker results are provided by NOAA-ESRL, Boulder, Colorado, USA through <http://www.esrl.noaa.gov/gmd/ccgg/carbontracker/>.

## References

- Aben, I., O. Hasekamp, and W. Hartmann (2007), Uncertainties in the space-based measurements of CO<sub>2</sub> columns due to scattering in the Earth's atmosphere, *J. Quant. Spectrosc. Radiat. Transfer*, *104*, 450–459.
- Bergamaschi, P., et al. (2007), Satellite cartography of atmospheric methane from SCIAMACHY on board ENVISAT: 2. Evaluation based on inverse model simulations, *J. Geophys. Res.*, *112*, D02304, doi:10.1029/2006JD007268.
- Bergamaschi, P., et al. (2009), Inverse modeling of global and regional CH<sub>4</sub> emissions using SCIAMACHY satellite retrievals, *J. Geophys. Res.*, *114*, D22301, doi:10.1029/2009JD012287.
- Berrisford, P., et al. (2009), The ERA-Interim archive, *ERA Rep. Ser. 1*, 16 pp., ECMWF, Reading, U. K.
- Bovensmann, H., J. Burrows, M. Buchwitz, J. Frerick, S. Noël, V. Rozanov, K. Chance, and A. Goede (1999), SCIAMACHY: Mission objectives and measurement modes, *J. Atmos. Sci.*, *56*, 127–150.
- Bril, A., S. Oshchepkov, and T. Yokota (2009), Retrieval of atmospheric methane from high spectral resolution satellite measurements: A correction for cirrus cloud effects, *Appl. Opt.*, *48*, 2139–2148.
- Butz, A., O. Hasekamp, C. Frankenberg, and I. Aben (2009), Retrievals of atmospheric CO<sub>2</sub> from simulated space-borne measurements of backscattered near-infrared sunlight: Accounting for aerosol effects, *Appl. Opt.*, *48*, 3322–3336.
- Butz, A., O. Hasekamp, C. Frankenberg, J. Vidot, and I. Aben (2010), CO<sub>4</sub> retrievals from space-based solar backscatter measurements: Performance evaluation against simulated aerosol and cirrus loaded scenes, *J. Geophys. Res.*, *115*, D24302, doi:10.1029/2010JD014514.
- Butz, A., et al. (2011), Toward accurate CO<sub>2</sub> and CO<sub>4</sub> observations from GOSAT, *Geophys. Res. Lett.*, *38*, L14812, doi:10.1029/2011GL047888.
- Dlugokencky, E., et al. (2009), Observational constraints on recent increases in the atmospheric CO<sub>4</sub> burden, *Geophys. Res. Lett.*, *36*, L18803, doi:10.1029/2009GL039780.
- Frankenberg, C., J. Meirink, M. Van Weele, U. Platt, and T. Wagner (2005), Assessing methane emissions from global space-borne observations, *Science*, *308*, 1010–1014.
- Frankenberg, C., et al. (2008), Tropical methane emissions: A revised view from SCIAMACHY onboard ENVISAT, *Geophys. Res. Lett.*, *35*, L15811, doi:10.1029/2008GL034300.
- Hamazaki, T., Y. Kaneko, A. Kuze, and K. Kondo (2005), Fourier transform spectrometer for greenhouse gases observing satellite (GOSAT), *Proc. SPIE Int. Soc. Opt. Eng.*, *5659*, 73.
- Hansen, P. (1992), Analysis of discrete ill-posed problems by means of the L-curve, *SIAM Rev.*, *34*, 561–580.
- Hasekamp, O., and A. Butz (2008), Efficient calculation of intensity and polarization spectra in vertically inhomogeneous scattering and absorbing atmospheres, *J. Geophys. Res.*, *113*, D20309, doi:10.1029/2008JD010379.
- Houweling, S., et al. (2005), Evidence of systematic errors in SCIAMACHY-observed CO<sub>2</sub> due to aerosols, *Atmos. Chem. Phys. Discuss.*, *5*, 3313–3340.
- Intergovernmental Panel on Climate Change (2007) *Climate Change 2007: The Physical Science Basis: Contribution of Working Group I to the Fourth Assessment Report of the Intergovernmental Panel on Climate Change*, edited by S. Solomon et al., Cambridge Univ. Press, Cambridge, U. K.
- Krol, M., et al. (2005), The two-way nested global chemistry-transport zoom model TM5: Algorithm and applications, *Atmos. Chem. Phys.*, *5*, 417–432.
- Kuze, A., H. Suto, M. Nakajima, and T. Hamazaki (2009), Thermal and near infrared sensor for carbon observation Fourier-transform spectrometer on the greenhouse gases observing satellite for greenhouse gases monitoring, *Appl. Opt.*, *48*, 6716–6733.
- Mao, J., and S. Kawa (2004), Sensitivity studies for space-based measurement of atmospheric total column carbon dioxide by reflected sunlight, *Appl. Opt.*, *43*, 914–927.
- Meirink, J., et al. (2006), Sensitivity analysis of methane emissions derived from SCIAMACHY observations through inverse modelling, *Atmos. Chem. Phys.*, *6*, 1275–1292.
- Meirink, J. F., P. Bergamaschi, and M. C. Krol (2008a), Four-dimensional variational data assimilation for inverse modelling of atmospheric methane emissions: Method and comparison with synthesis inversion, *Atmos. Chem. Phys.*, *8*, 6341–6353.
- Meirink, J.-F., et al. (2008b), Four-dimensional variational data assimilation for inverse modeling of atmospheric methane emissions: Analysis of SCIAMACHY observations, *J. Geophys. Res.*, *113*, D17301, doi:10.1029/2007JD009740.
- O'Brien, D., and P. Rayner (2002), Global observations of the carbon budget: 2. CO<sub>2</sub> column from differential absorption of reflected sunlight in the 1.61 μm band of CO<sub>2</sub>, *J. Geophys. Res.*, *107*(D18), 4354, doi:10.1029/2001JD000617.
- Parker, R., et al. (2011), Methane observations from the greenhouse gases observing satellite: Comparison to ground-based TCCON data and model calculations, *Geophys. Res. Lett.*, *38*, L15807, doi:10.1029/2011GL047871.
- Patra, P., Y. Niwa, T. Schuck, C. Brenninkmeijer, T. Machida, H. Matsueda, and Y. Sawa (2011), Carbon balance of South Asia constrained by passenger aircraft CO<sub>2</sub>, *Atmos. Chem. Phys.*, *11*, 4163–4175, doi:10.5194/acp-11-4163-2011.
- Peters, W., et al. (2007), An atmospheric perspective on North American carbon dioxide exchange: CarbonTracker, *Proc. Natl. Acad. Sci. U. S. A.*, *104*, 18,925–18,930.
- Phillips, D. (1962), A technique for the numerical solution of certain integral equations of the first kind, *J. ACM*, *9*, 84–97.
- Remer, L. A., et al. (2005), The MODIS aerosol algorithm, products, and validation, *J. Atmos. Sci.*, *62*, 947–973.
- Schneising, O., M. Buchwitz, J. Burrows, H. Bovensmann, P. Bergamaschi, and W. Peters (2009), Three years of greenhouse gas column-averaged dry air mole fractions retrieved from satellite-Part 2: Methane, *Atmos. Chem. Phys.*, *9*, 443–465.
- Tikhonov, A. (1963), On the solution of incorrectly stated problems and a method of regularization, *Dokl. Acad. Nauk SSSR*, *151*, 501–504.
- Tran, H., and J. Hartmann (2008), An improved O<sub>2</sub>A band absorption model and its consequences for retrievals of photon paths and surface pressures, *J. Geophys. Res.*, *113*, D18104, doi:10.1029/2008JD010011.
- Wunch, D., et al. (2010), Calibration of the total carbon column observing network using aircraft profile data, *Atmos. Meas. Tech.*, *3*, 1351–1362.
- Wunch, D., G. Toon, J. Blavier, R. Washenfelder, J. Notholt, B. Connor, D. Griffith, V. Sherlock, and P. Wennberg (2011), The total carbon column observing network, *Philos. Trans. R. Soc. A*, *369*, 2087–2112.
- Yokota, T., H. Oguma, I. Morino, A. Higurashi, T. Aoki, and G. Inoue (2004), Test measurements by a BBM of the nadir-looking SWIR FTS aboard GOSAT to monitor CO<sub>2</sub> column density from space, *Proc. SPIE Int. Soc. Opt. Eng.*, *5652*, 182.
- Yoshida, Y., Y. Ota, N. Eguchi, N. Kikuchi, K. Nobuta, H. Tran, I. Morino, and T. Yokota (2011), Retrieval algorithm for CO<sub>2</sub> and CO<sub>4</sub> column abundances from short-wavelength infrared spectral observations by the greenhouse gases observing satellite, *Atmos. Meas. Tech.*, *4*, 717–734.